EUROPEAN ORGANIZATION FOR NUCLEAR RESEARCH
European Laboratory for Particle Physics
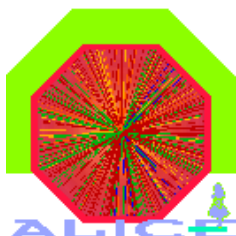
Evaluation of the performance of a magnetic drive gear pump in a magnetic field

Authors:

C. Pastore [1], I. Sgura [2]

(1) Università di Bari and INFN sez. Bari, Italy
(2) Politecnico di Bari and INFN sez. Bari, Italy

Abstract:

The aim of this paper is to report the influence of an external magnetic field on the performance of the MICROPUMP magnetic drive gear pump that has been adopted to serve in the C_6F_{14} liquid system of the ALICE HMPID detector. The external magnetic field generates on the pump shaft a torque which depends on the orientation and the strength of the field. This torque has to be added to the one required for the conversion of the mechanical energy into hydraulic energy. From the electrical point of view, at fixed motor speed, the total torque could increase until the absorbed energy power does not exceed the rate value. The experimental results demonstrated that the increase of the magnetic field strength does not change significantly the hydraulic performance, whereas it causes a progressive worsening of the electrical performance of the motor. The pump showed normal functioning under 350 Gauss, in agreement with the manufacturer's specifications.

Evaluation of the performance of a magnetic drive gear pump in a magnetic field

Table of Contents

1 Introduction

A liquid system, being installed in the UX25 and CR5, continuously supplies purified C_6F_{14} (perfluorohexane) to the ALICE HMPID detector [1].

Since most of the HMPID liquid system [2] is located in areas which will not be accessible during the LHC running period, it has been designed to have as few active components as possible. One of these is a magnetic drive gear pump [3] which is placed in UX25, near the solenoid door, on side A, where the measured value of magnetic field [4] is about 300 Gauss.

Due to the fact that the manufacturer does not provide the performance curve when the pump is operated with C_6F_{14} in the presence of the magnetic field, several tests were carried out reproducing the expected working conditions.

In order to reach a level of knowledge that guarantees a correct functioning of the pump during the experiment data taking, the head capacity, the displacement and efficiency of the pump have been investigated. In the following, the fundamental parameters which allow the characterization of a pump, the apparatus setup and test procedure will be presented, before discussing the results of the test and the conclusions.

2 Pumping system basics: the relationship between power and efficiency

In this paragraph some basic relationships between power and efficiency will be introduced for the main active components of the pumping system.

In order to classify the pumps, for a given hydraulic performance, the fluid mechanical literature refers to the overall pump efficiency (OPE) which takes in account the pump relative power losses. This parameter is obtained by comparing the fluid output power to the input power as follows:

$$\eta_p = Output\ /\ Input = P_f\ /\ P_s \tag{1}$$

where P_f is the net pumped hydraulic power defined as the product (Eq. 2) of the volumetric flow rate Q, the outlet head H, and the fluid specific weight γ

$$P_f\ =\ QH\gamma \tag{2}$$

P_s is the shaft input mechanical power given by the product of the rotational motor speed ω and torque T (Eq. 3):

$$P_s\ =\ \omega T \tag{3}$$

As consequence of the gear technology (see figure 1 in Appendix) the pump shaft power is different from the motor shaft one (power to drive the gear pump) whose ratio is defined as η_{m1}, whereas the efficiency of the motor η_{m2} is obtained by dividing the motor shaft power (P_r) to the motor electric input power (P_e).

$$\eta_{m1} = Ps\ /\ Pr \tag{4}$$

$$\eta_{m2} = P_r\ /\ P_e \tag{5}$$

Note: for alternate current and balanced 3-phase condition, the motor input power results to be $P_e = \sqrt{3}\, V\, I\, cos\phi$.

3   Layout of the hydraulic test

3.1   The experimental setup

The experimental tests were performed at CERN, in the building 168, using the magnet MNP17 which is able to produce a magnetic field in the range 0-1000 Gauss.
The apparatus consisted of a closed loop system, as shown in figure 2, in which the MICROPUMP magnetic drive gear pump model GC–M25JBS6 (Fig.1) drew the fluid (C_6F_{14}) from the tank (T1, 50 l volume) and pumped it through the discharge pipe back into the same tank.
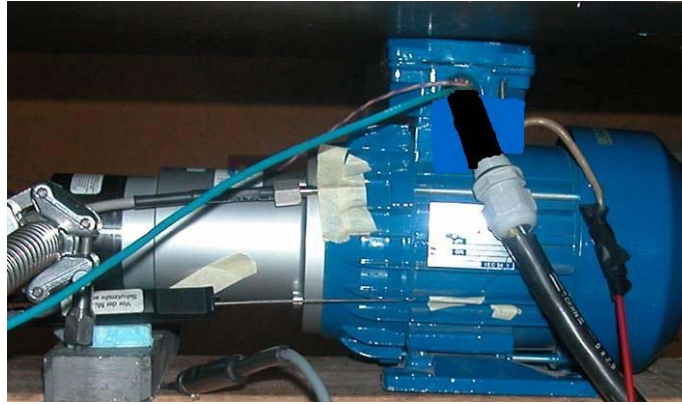
Fig.1 Magnetic drive gear pump GC–M25JBS6

The testing line has been equipped with several measuring devices assuring a high performance and accuracy. The fluid level inside the tank was monitored by means of a glass piezometer and the pressure by means of a pressure transmitter (PT1) which also allowed evaluating the pump suction head .
A second pressure transmitter (PT2) and a manometer (M1), as a redundant back up, measured the pressure at the output of the pump, whereas a mass flow meter (FM1) controlled the circuit flow rate.
The working point of the pumping system was set by means of a check valve (V1), located just downstream the pump outlet section . A pressure relief valve (that opens at a pressure of 10 mbar), two lines with a cold trap CT1 to recuperate the vapour perfluorohexane and a bubbler BB1 were installed at the top of the tank T1. A PT100 (TT1) was connected to CT1 for measuring the temperature of the liquid. The distance between the hydraulic instruments and the control sections (check valve, bend and pump) was fixed in compliance with the Hydraulic Institute rules [5].
The load efficiency of the motor of the pump was checked by measuring the power consumption and the temperature by means of, respectively, a digital ampere meter (A1) on the motor power supply line and a PT100 probe (TT2) installed on the motor frame. A digital gauss meter (G1) measured the magnetic field strength.
The main characteristics of the sensors are listed in Table 1 (Appendix).

During some tests a black steel tube (CERN SCEM code 39.23.05.216.5) was used to shield the pump motor against the external magnetic field.
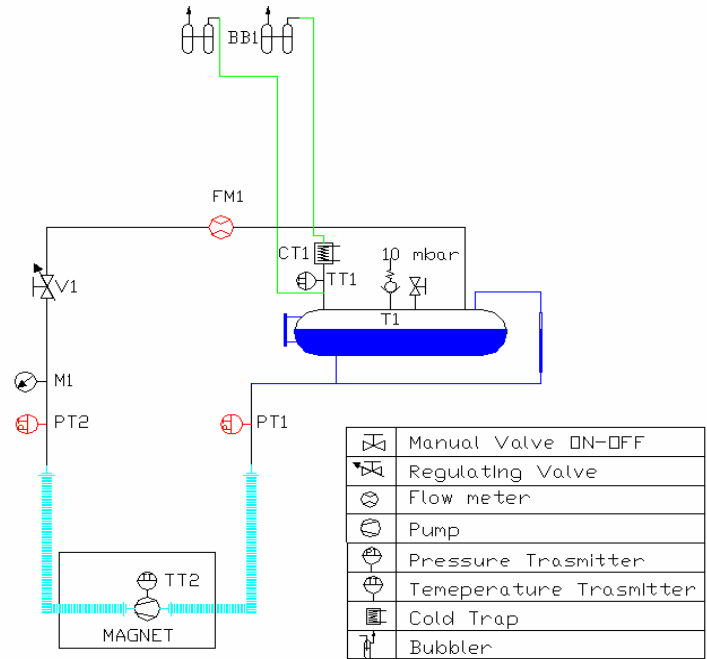

Fig. 2 Layout of the hydraulic experimental apparatus setup.

In order to monitor and to record the values of the pressure and temperature, the devices PT1, PT2 and TT1 were connected to a PLC Siemens S7 300 controlled via a PVSS interface (fig. 3a).
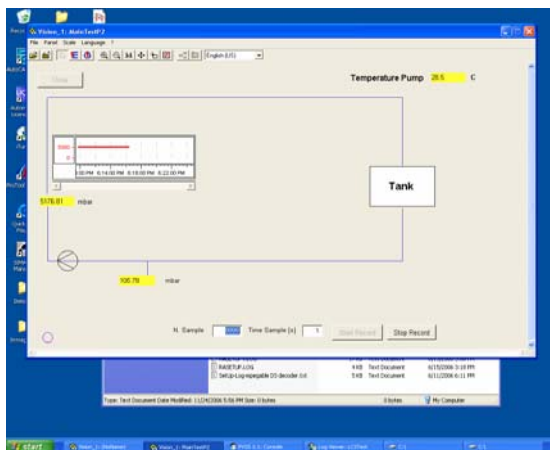

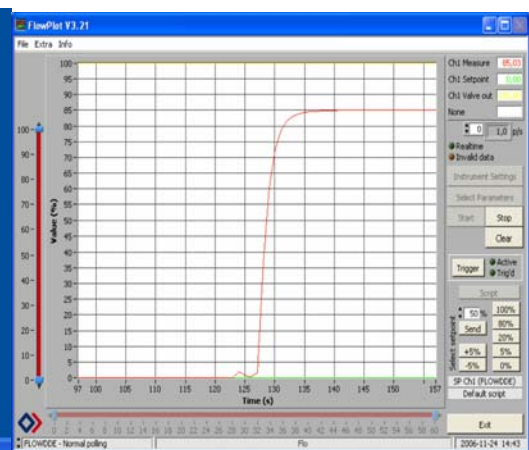*Fig. 3a The used PVSS interface.*   *Fig. 3b The used FlowPlot interface.*

The flow meter was directly connected to a laptop via RS232 and controlled through the appropriate software, FlowPlot (fig. 3b), whereas the nominal current, the values of the magnetic field and the temperature of the liquid were directly read by means of on the sensors display.

The sensors were powered at 24 V, the PLC at 220 V whereas the motor pump at 380V.

3.2   Test procedure

In order to guarantee the correctness and repeatability of the tests, an experimental protocol was established to fix the sequence of operations.

The normal test procedures started by setting the valve V1 at the desired opening, in order to set the required pressure and hence the required initial flow condition (the allowed minimum pressure was 4,5 bar owing to the pressure drop through FM1).

Once the opening ratio of the valve was fixed, the magnetic field value was increased from 0 until 500 Gauss. These actions were carried out for all configurations as detailed in the table 1 and showed in figure 4.

	No shielding	shielding	Orientation of the motor's axis
Configuration **A**	●		$\in \Pi xy$ // X
Configuration **B**		●	$\in \Pi xy$ // X
Configuration **C**	●		$\in \Pi xy$ // Y
Configuration **D**	●		$\in \Pi xz$ $\angle 45°$

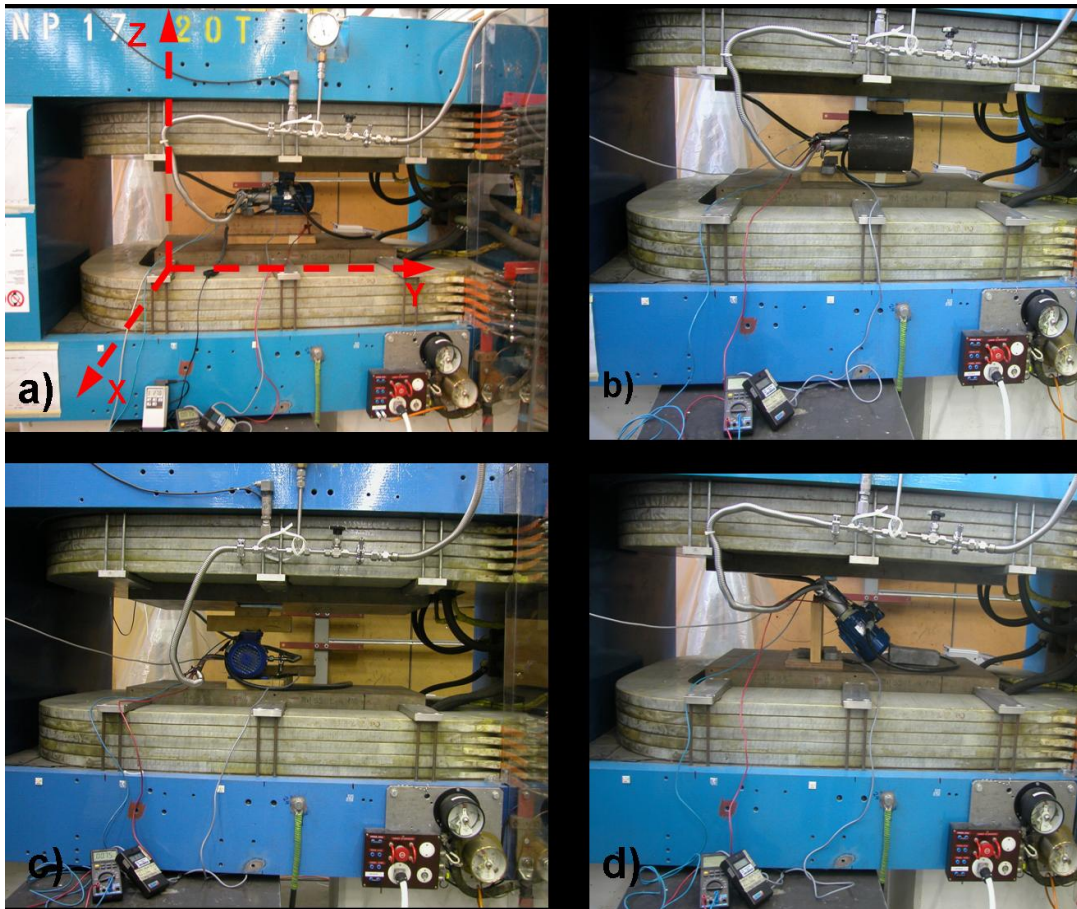*Table 1   Details of the testing configurations.*

Fig. 4 The pump in different spatial orientations. a) Configuration A; b) Configuration B; c) Configuration C; d) Configuration D

In order to verify whether the collected data were reproducible, each test was repeated three times.

During each measurement, after ensuring the steadiness flow field , the upstream and downstream pump pressure, the flow rate, the temperature of the liquid (to calculate its density, viscosity and vapour pressure according to [6]), the power consumption and motor temperature were recorded as specified above.

It must be stressed that the absence of cavitation at the inlet of the pump was always guaranteed during the test by the chosen position of the tank (Fig. 5), always ensuring the following energy condition:

$$NPSH_A \geq NPSH_R \qquad\qquad\qquad (6)$$

In other words, the amount by which the pressure in the pump inlet exceeds the liquid vapour pressure (Net Positive Section Head Available) should be higher than that required (Net Positive Section Head Required) by the characteristics of the pump design [7].

Fig. 5 Overview of the experimental setup.

4 Results and discussions

In the following, the results of the tests, as summarised in the figure 6 to 13 will be discussed. In figure 6 data has been collected in the form of hydraulic curves in which the output head H is plotted against flow rate Q, in the configuration A and B.
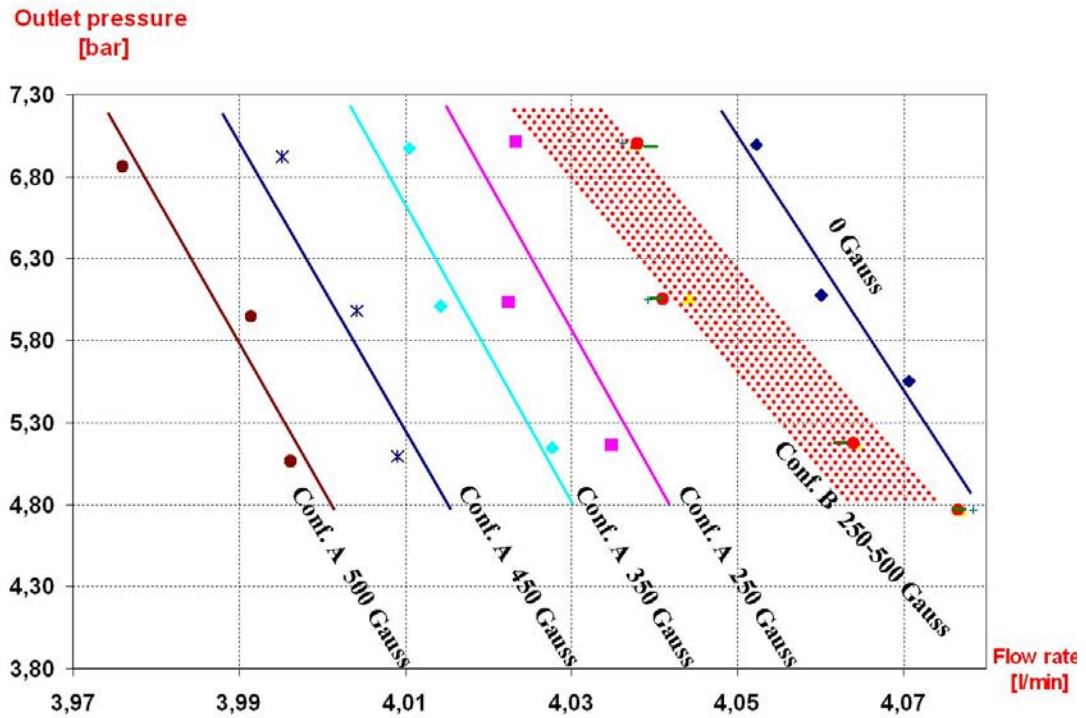
Fig. 6 Hydraulic performance curves of the pump for the different configurations.

Observing the figure 6 it is clear that, in configuration A, the hydraulic performance is in inverse relation to the magnetic field value, whereas in the configuration B it is noted a different performance between absence and presence of magnetic field, but the same behaviour from 250 to 500 Gauss
It must be said that, in all configurations, the decay of the hydraulic performance is quite low, as shown in figure 7 reaching, a maximum value of about 3 % in configuration A and of about 0.5 % in the configuration B, when a 500 Gauss magnetic field was set.
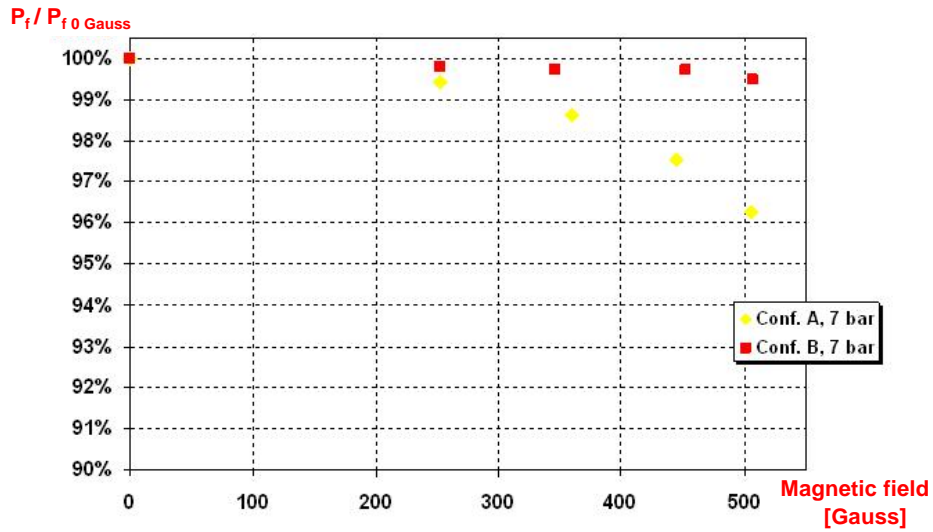
Fig.7 Hydraulic energy vs the magnetic field strength at fixed output pressure.

On the other hand, figure 8 shows that the worsening of the motor working conditions, by increasing of the magnetic field, is not negligible since the absorbed current I_a and hence the absorbed power P_e, increases.

In particular, in all tested conditions, I_a increases from 0,74 A to 1.2 A when the magnetic field grows from 0 to 500 Gauss for configuration A, whereas, for configuration B, I_a remains quite constant and equal to 0,74 A for magnetic field values lower than 350 Gauss and increases until 0,83 A when the magnetic field values exceed 350 Gauss.
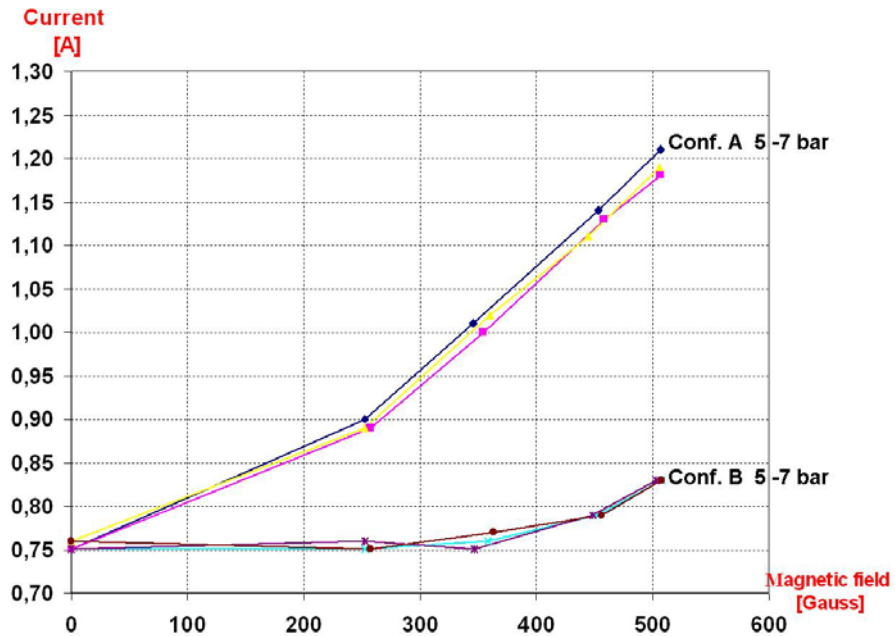

Fig. 8 The absorbed current vs the magnetic field in the configurations A and B at different flow conditions.

The motor rated power (P_{eN}), $\cos\phi_N$ and η_{m1}, P_r and hence P_s have been calculated, for each I_a value, using an iterative method and the tables provided by the manufacturer[8].

Figure 9 shows P_r as a function of the intensity of the magnetic field, at fixed pressure. It is clear that P_r and, as consequence, P_s is strongly affected by the magnetic field strength as expected (see eq. 3).

In fact the magnetic field generates on the pump shaft a torque T_m, proportional to the magnetic field strength, which has to be added to the torque T_h required for the conversion into hydraulic energy P_f.
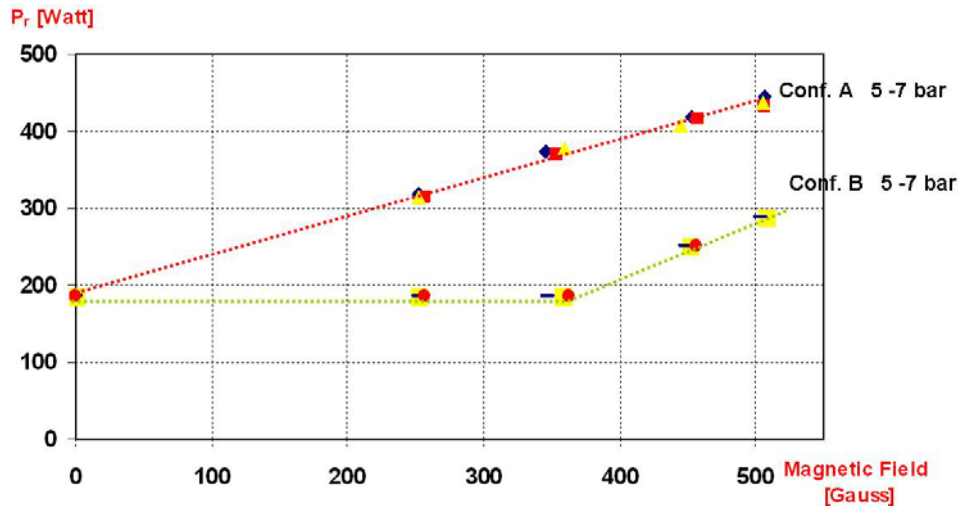

Fig.9 The motor shaft power vs the magnetic field in the configurations A and B at different flow conditions

It is also important to notice, as in configuration A, the increase of P_r is such that it exceeds the maximum value suggested by manufacturer (370 W) to avoid an increase of the motor temperature. As sketched in figure 10, the experimental data confirm the manufacturer reference: in fact, in the configuration A a temperature growth of about 25% is observed when the magnetic field changes between 0 and 500 Gauss, while this variation is only 2% in configuration B. Note: the maximum working temperature range was between 25°C and 35°C.
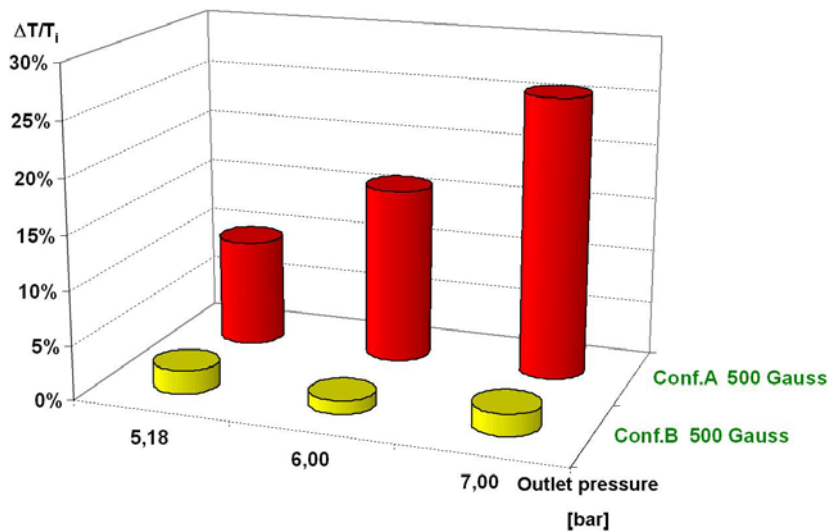

Fig.10 The variation of the temperature versus different flow condition, in the configurations A and B.

In order to complete the pump performance analysis, the overall pump efficiency η_P was calculated using equation (1). Comparing the plots (fig.11) of the η_P as a function of the magnetic field at the various conditions, all the above experimental evidences are confirmed and more highlighted.
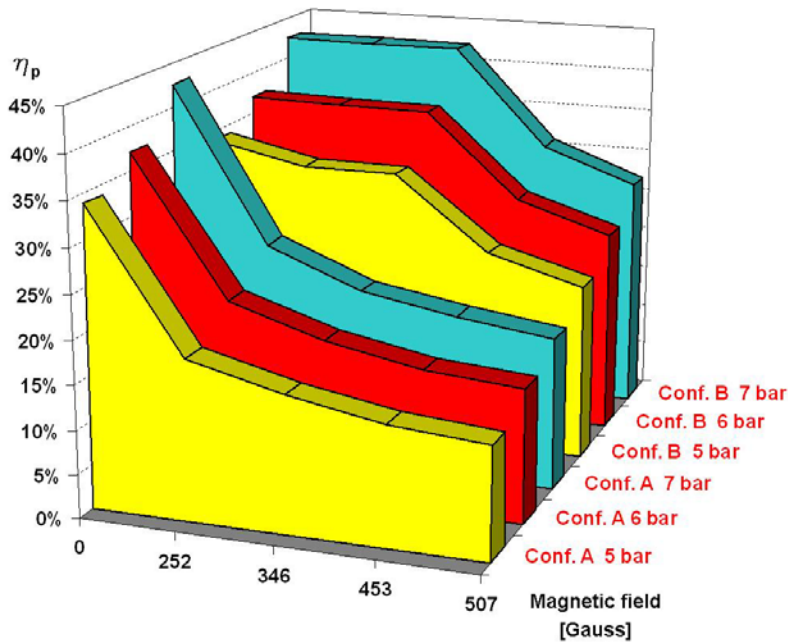

Fig.11 The overall pump efficiency vs the magnetic field in the configurations A and B at different flow conditions.

In the configuration A, the value η_P decreases with the increasing of the magnetic field, at fixed pressure, moreover in the configuration B the value of the η_P remains almost constant until 350 Gauss and then decreases.

All these results demonstrate a good shielding effect until about 350 Gauss.

The last data collected concern the study of the behavior of the pump in the C and D configurations (see table 1). Following the previous analysis the hydraulic curves H=H(Q) were reported (figure 12). As expected, nothing changes as long as the axis of the pump lays in the plane Πxy, perpendicular to the direction of the magnetic field (configuration A and C) while the trend in configuration D lays between the one for configuration A/C and B.

Figure 13 confirms the complete agreement with the previous considerations. In fact, modifying the spatial orientation of the motor axis, the additional torque T_m reaches a maximum value in the configuration A/C and a minimum one (toward to 0) when the motor axis is along the Z axis (see the fig.4). Therefore, since P_f remains almost constant, the pump efficiency η_P changes following the variation of T_m (equations (2) and (3)).
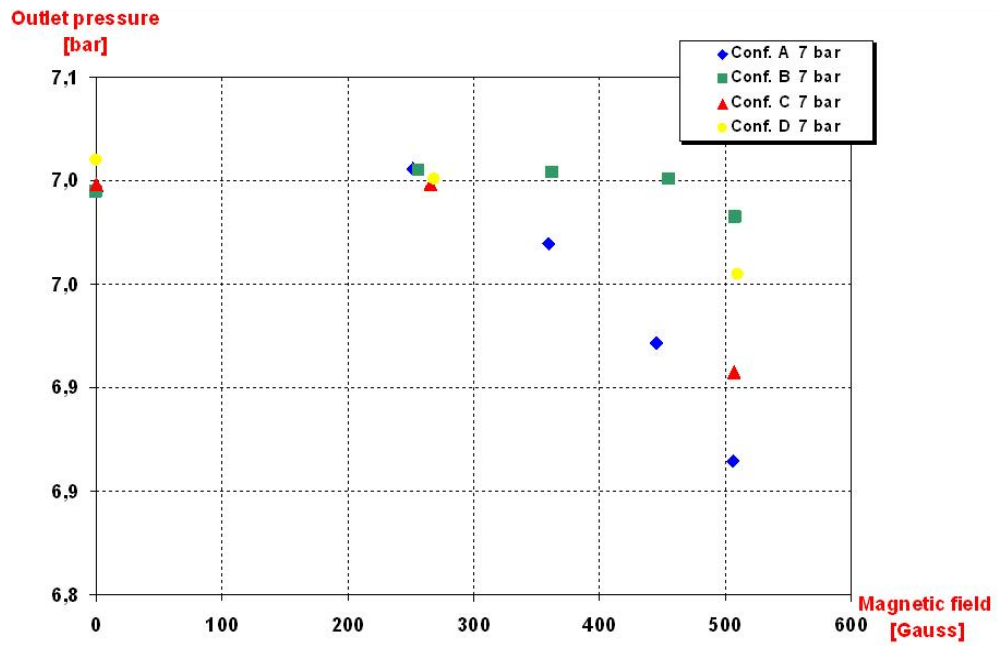
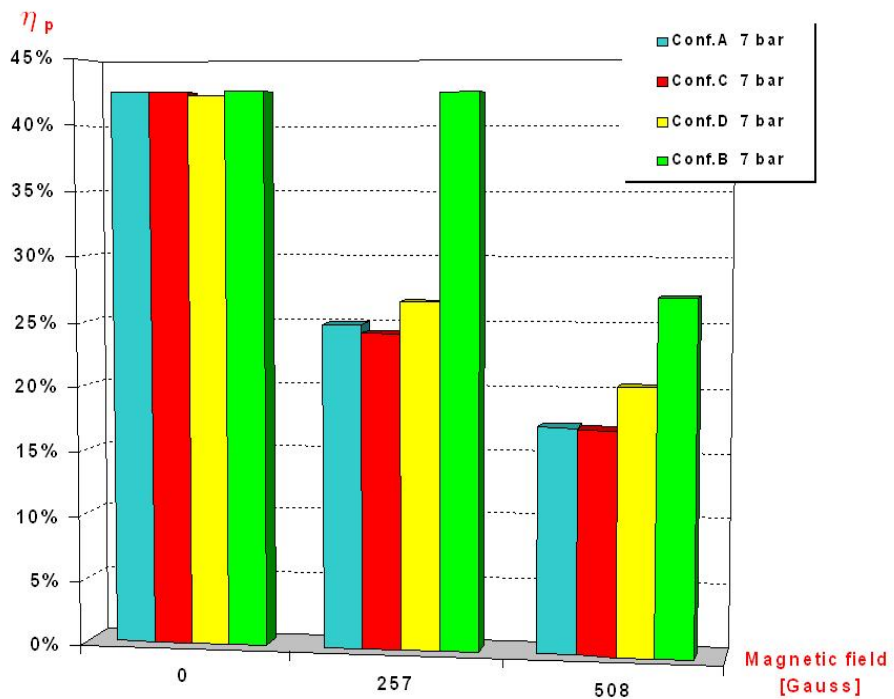*Fig. 12 Outlet pressure in a function of the magnetic field, in all configurations at fixed valve's opening.*

Fig. 13 Comparison of the efficiency of the pump in all configuration at fixed valve's opening.

Conclusions

The following conclusions summarize the results of the experimental investigations:

1) for all tested configurations the hydraulic energy produced by the pump does not change significantly, showing a little worsening with an increase of the magnetic field;
2) in the configurations A, C and D the absorbed power varies between 185 W and 450 W therefore exceeding the maximum value (370 W) suggested by the manufacturer;
3) in the configurations A, C and D, for fixed pressure, η_P decreases as the magnetic field increases, however in the configuration B it remains almost constant until 350 Gauss, and then it decreases.

On the basis of the results of the experimental tests performed in order to guarantee the correct functioning of the pump during the LHC operations, the use of a shielding is advisable being the expected magnetic field strength value close to the pump rack about 300 Gauss.
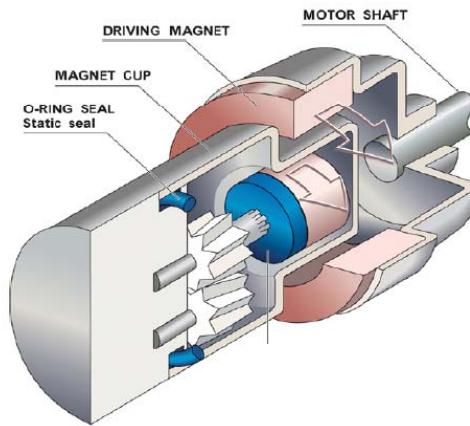
Appendix

Fig. 1 Cross section of a magnetic drive gear pump.

Component	Manufacturer	Range	Accuracy
PT1	Bourdon-Haenni	-1÷1 [bar]	± 0,25 % FS
PT2	Bourdon-Haenni	0÷10 [bar]	± 0,25 % FS
FM1	Bronkhorst	0÷500 [Kg/h]	± 1 % FS
TT1	n.a.	0÷100 [°C]	± (0.3+0.005*t) °C
TT1	Bourdon-Haenni	0÷100 [°C]	± (0.3+0.005*t) °C
A1	Escort	0÷10 [A]	± 1,5 % FS
G1	Maurer Magnetique	[0÷1000] [Gauss]	± 1 % FS

Table1 Main Characteristics of the used instruments

Acknowledgements

We would like to thank R.Rey-Mermier and Jacob Van Beelen of PH-DT1 for their help and technical support.

References:

[1] ALICE Collaboration, HMPID TDR, CERN/LHCC 98-19.

[2] ALICE Collaboration, *The HMPID C_6F_{14} circulation system*, ALICE-INT-2007-003 v. 1.0.

[3] **Steven E. Owen**, *Advantages of a magnetically driven Gear Pump,*
www.micro**pump**.com/pdfs/application%20notes/fea_art_advantages.pdf.

[4] **D.Swoboda, H.Taureg**, *Measurements of the Magnetic Stray Field for the ALICE Muon Dipole and L3 Solenoid*, ALICE-EN-2006-001.

[5] http://www.pumps.org/

[6] *3M™ Performance Fluid PF-5060DL*
http://multimedia.mmm.com/mws/mediawebserver.dyn?6666660Zjcf6lVs6EVs666x WiCOrrrrQ-

[7] **R.Rayner**, *Pump Users Handbook*, Elsevier Science Publishers LTD.

[8] http://www.elektropol-cantoni.com/pdf/rendimentog.pdf